Materials Advances

ROYAL SOCIETY OF CHEMISTRY

COMMUNICATION

View Article Online
View Journal | View Issue

Cite this: *Mater. Adv.*, 2020, **1**, 2712

Received 5th June 2020,
Accepted 2nd October 2020

DOI: 10.1039/d0ma00380h

rsc.li/materials-advances

Magnetic and thermal responses of a nonvolatile shape memory fluid†

Koji Tsuchiya, Yu Hagiwara, Makoto Nakagawa, Hiroshi Endo and Takeshi Kawai *

We report on a novel nonvolatile shape memory fluid derived from magnetic nanoparticles dispersed in water, oil, and oil/water emulsions. Magnetic fields are used to lock fluid shapes into place, even after the field is removed. Thermal treatments release the locked fluid back to its original shape.

1. Introduction

Shape memory is a type of memory that has the ability to write, store, and erase information in its shape by applying and removing an external stimulus, such as a voltage, light, heat, or a magnetic field.[1] Shape-memory polymers, which are one of the most enthusiastically researched shape memory materials, are stimuli-responsive (smart) polymers that change their chemical or physical properties, including shape, upon exposure to external stimuli.[1] The transformation of the original shape in shape-memory polymer systems requires a difficult mechanical process because, as a solid-based memory, changes in volume, length, or a bending action may be involved.

On the other hand, fluid-based shape memory has a great advantage in that a shape can be easily molded through an external stimulus.[2–4] Magnetic fluid, which is a stable colloidal suspension of ferromagnetic nanoparticles (NPs), is magnetized in the presence of a magnetic field. The original and transformed shape of the magnetic fluid can be changed by tuning the direction or intensity of a magnetic field.[3,4] However, the shape molded by the magnetic field is not retained when the magnetic field is removed, and unlike shape-memory polymers, it lacks the ability to retain its shape and behaves as a fluid. Another type of fluid consisting of a magnetic particle suspension, known as a magnetorheological (MR) fluid,[5] can solidify under a strong magnetic field, but its shape does not change when influenced by a magnetic field. The solidification is caused by a chain-like arrangement of the dispersed magnetic particles in the direction parallel to the applied magnetic field.

The deformable function of magnetic fluids and the solidification function of MR fluids are inactivated when magnetic fields are removed. An innovative and valuable nonvolatile shape memory fluid would combine the ability to mold a dispersion of magnetic NPs with the ability to retain the shape when the magnetic field is removed. Our research in this communication describes a novel nonvolatile magnetic shape memory fluid that affords writing, retention, and erasing of the fluid shape by a combination of magnetic fields and thermal treatments. Magnetic fluids suitable for nonvolatile shape memory devices contain magnetic Fe_3O_4 NPs covered with a surfactant, bis(aminoethyl-carbamoylethyl)-octadecylamine (C18AA, Fig. 1A),[6,7] that not only acts as a dispersant, but also as a base and reducing agent. There are several advantages to C18AA. First, its use as a surfactant also produces magnetic NPs in a simple one-step preparation process. C18AA also functions well as an organogelator in various organic solvents. In addition, it also can generate a heat-induced oil-in-water (O/W) emulsion gel,[6] which undergoes phase transitions from sol to gel on heating.

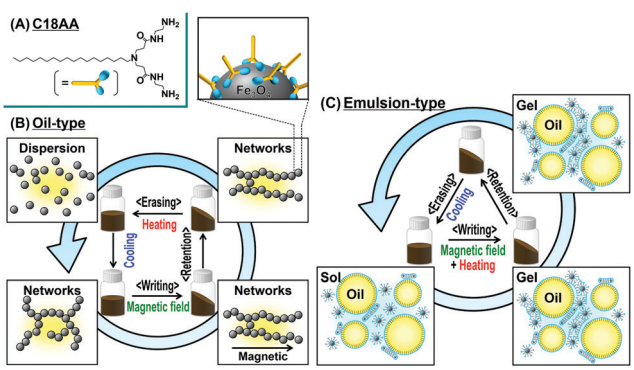

Fig. 1 (A) Chemical structure of C18AA. (B and C) Schematic illustration of nonvolatile shape memory with Fe_3O_4 NPs covered with C18AA dispersed in (B) oil and (C) an O/W emulsion.

Department of Industrial Chemistry, Tokyo University of Science, 1-3 Kagurazaka, Shinjuku, Tokyo 162-8601, Japan. E-mail: kawai@ci.kagu.tus.ac.jp

† Electronic supplementary information (ESI) available. See DOI: 10.1039/d0ma00380h

In this research, we have demonstrated that C18AA can be used to simply prepare oil-based (Fig. 1B) and O/W emulsion-based (Fig. 1C) magnetic fluids with nonvolatile shape memory properties. Even in the absence of magnetic fields, the magnetic fluid shapes created by the application of an external magnetic field were "fixed", or locked into place, by the thixotropy associated with the sol–gel transition behavior of the fluid with the added C18AA. Furthermore, we showed that the stabilized shapes can be converted back to their original rheology by either heating (Fig. 1B) or cooling (Fig. 1C), depending on whether the sol is oil-based or an O/W emulsion.

2. Results and discussion

Fe_3O_4 NPs were prepared by simply mixing $FeCl_2$ with C18AA in water at room temperature (see ESI†). The color of the obtained suspension varied from greenish to brown or to black, depending on the C18AA concentration. Homogeneous black dispersions were obtained at [C18AA] $\geq$ 200 mM, and these dispersions were stable for at least one month. On the other hand, phase separation occurred within a few minutes with [C18AA] $\leq$ 100 mM, and a brown and black phase precipitated out. The color change suggests the formation of iron oxide NPs.

Fig. 2A and B show typical transmission electron microscopy (TEM) images of the resulting NPs at C18AA concentrations of (A) 50 mM and (B) 200 mM, respectively. The TEM micrographs revealed that raspberry-like agglomerates of the NPs with diameters of approximately 60 nm were obtained at [C18AA] = 50 mM, while NP clusters approximately 15 nm in diameter consisting of fused smaller NPs ($\sim$7 nm) were obtained at [C18AA] = 200 mM. Powder X-ray diffraction (XRD) data (Fig. 2C) revealed diffraction patterns that corresponded to Fe_3O_4 with a face-centered cubic (FCC) structure for the latter NPs, while the former NPs had diffraction patterns that corresponded to both Fe_3O_4 and β-FeOOH. These TEM and XRD results indicate the formation of Fe_3O_4 NPs without β-FeOOH at [C18AA] $\geq$ 200 mM in the present system.

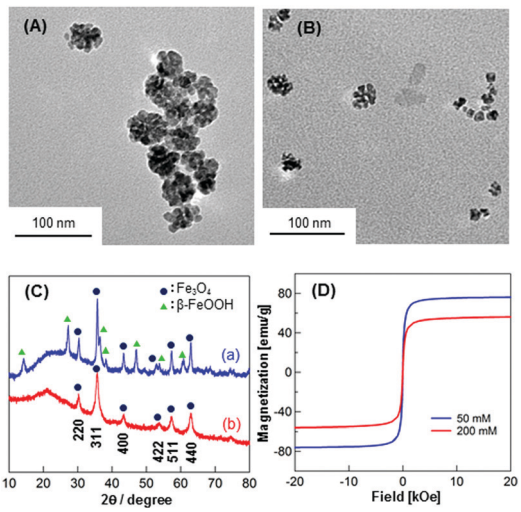

Fig. 2 Typical TEM micrographs of NPs obtained at (A) [C18AA] = 50 mM and (B) 200 mM. (C) XRD patterns of NPs obtained at (a) [C18AA] = 50 mM and (b) 200 mM. (D) Superimposed hysteresis curves for NPs obtained at [C18AA] = 50 mM and 200 mM after washing with ethanol.

The magnetic properties of the Fe_3O_4 NPs were investigated using a superconducting quantum interference device (SQUID) magnetometer. Fig. 2D shows hysteresis loops for Fe_3O_4 NPs after washing with ethanol to remove C18AA. The lack of hysteresis in Fig. 2D indicated that the obtained Fe_3O_4 NPs exhibit typical superparamagnetic properties. Under a large external field, the magnetization aligned with the field direction and reached saturation. The saturation magnetization values were 75 and 56 emu g^{-1} for Fe_3O_4 NPs prepared with [C18AA] = 50 and 200 mM, respectively. The difference in saturation magnetization is mainly caused by the difference in the size of the NPs. The saturation magnetization values were lower than those of similarly-sized NPs prepared by other methods,[8] which may be caused by surface spin-canting effects induced by the terminal amine groups of C18AA on the NPs.[9] Zero-field cooled (ZFC) and field cooled (FC) magnetization curves (Fig. S1, ESI†) also revealed the superparamagnetism of the obtained Fe_3O_4 NPs.

There have been several approaches to the synthesis of Fe_3O_4 NPs.[8,10] In most of the previous reports, the preparation of magnetic NPs has required a complicated multistep process, and adjustment to an appropriate pH or a relatively high temperature (>200 °C). In contrast, magnetic Fe_3O_4 NPs have been prepared here by a facile process that involves mixing $FeCl_2$ with C18AA in water at room temperature.

The Fe_3O_4 NPs obtained were stably dispersed in water over a wide range of pH values (pH 2–11). Zeta-potential measurements of the Fe_3O_4 NP dispersions (Fig. S2, ESI†) indicated that the isoelectric point for Fe_3O_4 NPs dispersed with C18AA was at a high pH value of approximately 11, compared to a pH of 7 for the Fe_3O_4 NP dispersion without C18AA,[11] and the ζ-potentials were maximized (>20 mV) at pH < 11. This high ζ-potential can be ascribed to the high stability of the dispersions over a wide pH range of 2–11. Furthermore, because Fe_3O_4 NP dispersed with C18AA had the higher ζ-potentials than those without C18AA, it is likely that the Fe_3O_4 NPs were covered with cationic surfactant molecules of C18AA. The interaction between C18AA and Fe_3O_4 NPs was also confirmed by X-ray photoelectron spectroscopy (XPS) measurements (Fig. S3, ESI†). The N 1s XPS peak at 399.6 eV for pure C18AA was shifted to a higher value (399.9 eV) for NPs with C18AA, which suggests that the terminal amine groups of C18AA act as a somewhat charged species.[9]

The magnetic properties of the fluids were investigated by moving a 510 mT neodymium magnet close to the dispersions of Fe_3O_4 NPs in water prepared with various concentrations of C18AA. Interestingly, the as-prepared homogeneous Fe_3O_4 dispersions ([C18AA] $\geq$ 200 mM) were attracted to the magnet (Fig. 3B). In contrast, the unstable dispersions (demonstrating phase separation and precipitation) prepared with [C18AA] $\leq$ 100 mM did not exhibit magnetic fluid properties (Fig. 3A), although a part of the precipitate was attracted to the magnet, because the resultant NPs consisted of a mixture of magnetic Fe_3O_4 and non-magnetized β-FeOOH.

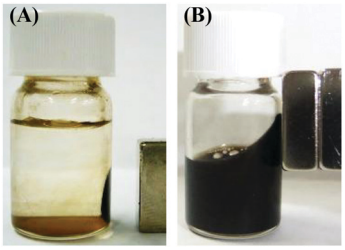

Fig. 3 Photographs of Fe_3O_4 NP dispersions in water prepared at (A) [C18AA] = 50 mM and (B) 200 mM when a neodymium magnet approaches the dispersions.

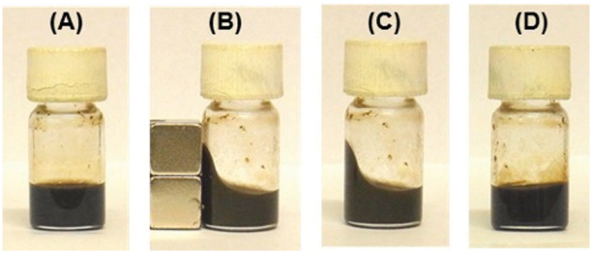

Fig. 4 Photographs of Fe_3O_4 NPs dispersed in toluene. (A) Before and (B) after the dispersion is placed in the proximity of a neodymium magnet at room temperature. (C) Sample (B) after removal of the magnet at room temperature. (D) Sample (C) after heating above 40 °C.

C18AA has been reported to have the potential to disperse NPs[7a,b] or carbon nanotubes[12] in both organic solvents and water, indicating that organic solvent-based magnetic fluids could be prepared from a water-based magnetic fluid. After the water was evaporated from the water-based magnetic fluid under reduced pressure, several different organic solvents were added to the residue of Fe_3O_4 NPs and C18AA. Homogeneous organic solvent dispersions of Fe_3O_4 NPs were obtained by vigorous agitation and subsequent sonication. Stable dispersions of the Fe_3O_4 NPs were easily prepared in toluene, benzene, and even in an ionic liquid, 1-hexyl-3-methylimidazolium chloride, while dispersions in hexane, cyclohexane, and tetrahydrofuran (THF) were reasonably stable only for a few hours. In contrast, the dispersions in chloroform and methanol were unstable, and Fe_3O_4 NPs completely precipitated within an hour. The difference in the dispersibility is probably related to the solubility of C18AA in the solvents. Chloroform and methanol are very good solvents for C18AA, which causes the desorption of C18AA from the surface of the Fe_3O_4 NPs. However, the other solvents do not have a high solvation power for C18AA, indicating that the Fe_3O_4 NP surfaces may remain saturated with C18AA to afford a stable dispersion.

Fig. S4 and S5 of the ESI† show flow curves and viscosity curves for the Fe_3O_4 NP dispersions in various solvents. The flow curves in hexane, cyclohexane, and THF exhibited non-Bingham fluid behavior: non-linear curves having a yield stress. However, the flow curves of toluene and benzene corresponded to pseudoplastic fluid behavior. These dispersions behaved as non-Newtonian fluids and had thixotropic properties. In contrast, the dispersion in water was a Newtonian fluid, in which the shear stress is proportional to the shear rate. Further, viscosity measurements revealed that all organic solvent-type magnetic fluids investigated in the present study had shear thinning properties, a characteristic of thixotropy. In the case of the water-type magnetic fluid, the viscosity was independent of the shear rate.

All of the stable dispersions, including the ionic liquid, exhibited magnetic fluid properties, although the strength of the magnetic response was dependent on the solvent type. The gel-state of dispersions consisting of Fe_3O_4 NPs and C18AA in hexane, cyclohexane, toluene, benzene, and THF, which are poor solvents for C18AA, acted as a magnetic fluid with thixotropic properties (Table S1 and Fig. S6, ESI†). Fig. S7 of the ESI† summarizes the appearance of the oil-based magnetic fluids when an external magnetic field was applied, in addition to the dispersibility, dispersion state, and thixotropy.

The shape of the dispersion induced by an external magnetic field was fixed simply by keeping the dispersion at room temperature, even when the magnetic field was removed (Fig. 4A–C). Fixation of the magnetic fluid dispersions required a short time of 10 min under the magnetic field at room temperature. Further, the fixed dispersions could easily be made to flow again by heating above 40 °C (Fig. 4D), and the fixed and fluidized states of the organic dispersions were completely reversible many times.

This shape-memory behavior is ascribed to a change in the aggregation state of Fe_3O_4 NPs by the application of magnetic and thermal stimuli. As the schematic illustration of the oil-based magnetic fluid behavior shows in Fig. 1B, Fe_3O_4 NPs are probably aggregated to form three-dimensional networks due to the intermolecular attraction of C18AA molecules adsorbed on the Fe_3O_4 surface, which results in the gel state of the dispersion. When the dispersion is placed in the proximity of a magnet, the magnetic NPs align to form chain-like networks in the direction parallel to the magnetic field, which induces the shape deformation. The molded shape can be fixed due to interparticle attraction, even after removal of the magnetic field. Subsequent heating of the fluid causes destruction of the chain-like networks of Fe_3O_4 NPs, which results in a decrease in viscosity and a return to the original shape.

We have previously reported that O/W emulsions of C18AA resulted in a heat-induced gel that undergoes a thermal phase transition from a sol state to a rigid gel-like state upon heating.[6] From these results, we surmised that O/W emulsion-based magnetic fluids may be feasible. Fig. 5A shows an optical micrograph of a dispersion consisting of C18AA/toluene/water containing 0.1 M HCl to accelerate the gelation process at room temperature. In this system, the weight percent concentration of C18AA is defined as $[C18AA]_w$ (see ESI†), assuming that all C18AA molecules are present in the water phase. In the case of the dispersion shown in Fig. 5A, $[C18AA]_w$ was 23 wt%. The optical micrograph shows that toluene droplets with diameters of several micrometers were obtained, indicating demulsification of the fluid into the toluene and water phases. Because Fe_3O_4 NPs were present in the water phase when the emulsion was demulsified, Fe_3O_4 NPs were dispersed by C18AA in the continuous phase of water.

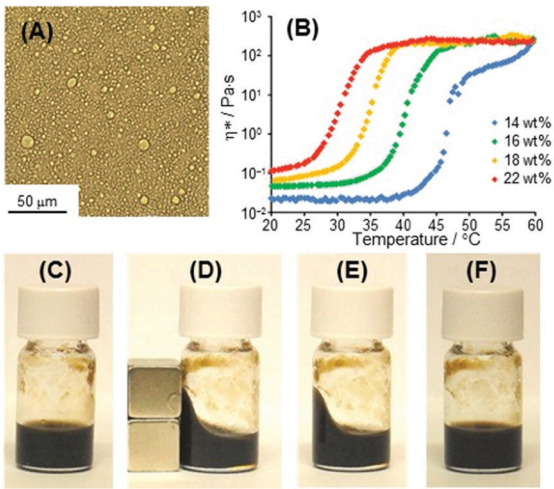

Fig. 5 (A) Optical micrograph of the dispersion consisting of C18AA/toluene/water containing 0.1 M HCl. $[C18AA]_w$ = 23 wt% and a 6 : 4 volume ratio of oil to water. (B) Complex viscosity (η^*) as a function of temperature for the O/W emulsion-type magnetic fluids prepared at various [C18AA]w and with toluene as the organic solvent. (C–F) Photographs of the O/W emulsion-type magnetic fluid prepared at $[C18AA]_w$ = 18 wt%. (C) Before and (D) after the dispersion is placed in the proximity of a neodymium magnet at room temperature. (E) After the dispersion is allowed to stand at 40 °C followed by removal of the magnet. (F) After sample (E) is cooled to room temperature.

The thermal response of the O/W emulsions containing Fe_3O_4 NPs was examined by measuring the complex viscosity η^*, obtained from the storage (G') and loss (G'') moduli as a function of temperature (Fig. 5B). η^* for the O/W emulsions containing Fe_3O_4 NPs prepared with $[C18AA]_w$ = 18 wt% changed from approximately 8×10^{-2} to 250–350 Pa s upon heating, accompanied by a sol-to-gel phase transition at 34 °C. Our previous study on O/W emulsion systems prepared with C18AA but without Fe_3O_4 NPs indicated that oil droplets covered with C18AA coexist with spherical or short rod-like micelles of C18AA in water at low temperatures. An increase in temperature induces the growth of micelles into elongated micelles, which causes an increase in viscosity.[6] Therefore, the heat-induced gelation of the present O/W emulsion-based magnetic fluid is most likely caused by a similar mechanism. The thermal viscosity behavior affords heat-gelation and cool-softening properties to the O/W emulsion-based magnetic fluid, and the change in viscosity upon heating and cooling was completely reversible many times. This enables the magnetic fluid shape to be molded with an external magnetic field at temperatures greater than the sol–gel transition temperature. When a magnet was used to change the shape of the emulsion-based magnetic fluid, the shape could be fixed in the sol state by heating above the sol–gel transition temperature to form a gel with a high viscosity (Fig. 5C–E). In addition, the temperature of shape fixation, *i.e.*, the sol–gel transition temperature, was a function of the C18AA concentration. Fig. 5B shows that as $[C18AA]_w$ concentration decreased from 24 to 14 wt%, the temperature at which the shape was fixed increased from approximately 27 °C to 45 °C, Furthermore, the deformed fluid shape induced by a magnetic field was easily returned to the original viscosity by cooling to room temperature (Fig. 5F).

3. Conclusions

In summary, we have demonstrated that magnetic Fe_3O_4 NPs were prepared by a facile process that involves mixing $FeCl_2$ with C18AA in water at room temperature. Various types of Fe_3O_4 NP dispersions in water, oil, and an O/W emulsion were investigated. Using C18AA with the magnetic Fe_3O_4 NPs in both oil and an oil/water emulsion enabled us to achieve a functional nonvolatile shape memory fluid. An applied magnetic field was used to fix the shape of the memory fluid, and for the oil-based system, the application of heat returned the fluid viscosity to its original value. In contrast, cooling the fixed shape of the memory fluid fabricated in an oil/water emulsion also returned the fluid viscosity to its original value. The system reported here is a promising candidate as new nonvolatile shape memory for various technological applications such as magnetic inks and actuators, because the rheological behavior can be controlled by both a magnetic field and temperature.

Conflicts of interest

There are no conflicts of interest to declare.

Notes and references

1 (*a*) H. Meng and G. Li, *Polymer*, 2013, **54**, 2199–2221; (*b*) S. Zhang, A. M. Bellinger, D. L. Glettig, R. Barman, Y.-A. L. Lee, J. Zhu, C. Cleveland, V. A. Montgomery, L. Gu, L. D. Nash, D. J. Maitland, R. Langer and G. Traverso, *Nat. Mater.*, 2015, **14**, 1065–1071; (*c*) Z. Yang, Q. Wang and T. Wang, *ACS Appl. Mater. Interfaces*, 2016, **8**, 21691–21699.
2 A. Groisman, M. Enzelberger and S. R. Quake, *Science*, 2003, **300**, 955–958.
3 Y. Zhang and N. T. Nguyen, *Lab Chip*, 2017, **17**, 994–1008.
4 (*a*) U. Banerjee and A. K. Sen, *Soft Matter*, 2018, **14**, 2915–2922; (*b*) D. Tian, N. Zhang, X. Zheng, G. Hou, Y. Tian, Y. Du, L. Jiang and S. X. Dou, *ACS Nano*, 2016, **10**, 6220–6226; (*c*) C. Rigoni, M. Pierno, G. Mistura, D. Talbot, R. Massart, J. C. Bacri and A. Abou-Hassan, *Langmuir*, 2016, **32**, 7639–7646.
5 (*a*) J. de Vicente, D. J. Klingenberg and R. Hidalgo-Alvarez, *Soft Matter*, 2011, **7**, 3701–3710; (*b*) K. Shahrivar and J. de Vicente, *Soft Matter*, 2013, **9**, 11451–11456; (*c*) P. J. Rankin, J. M. Ginder and D. J. Klingenberg, *Curr. Opin. Colloid Interface Sci.*, 1998, **3**, 373–381; (*d*) B. Bharti, A.-L. Fameau, M. Rubinstein and O. D. Velev, *Nat. Mater.*, 2015, **14**, 1104–1109.
6 C. Morita, H. Sugimoto, K. Matsue, T. Kondo, Y. Imura and T. Kawai, *Chem. Commun.*, 2010, **46**, 7969–7971.
7 (*a*) Y. Imura, C. Morita, H. Endo, T. Kondo and T. Kawai, *Chem. Commun.*, 2010, **46**, 9206–9208; (*b*) Y. Imura, H. Tanuma, H. Sugimoto, R. Ito, S. Hojo, H. Endo, C. Morita and T. Kawai, *Chem. Commun.*, 2011, **47**, 6380; (*c*) C. Morita, T. Aoyama, Y. Imura and T. Kawai, *Chem.*

Commun., 2011, **47**, 11760–11762; (*d*) M. Nakagawa, S. Watanabe, Y. Imura, K.-H. Wang and T. Kawai, *J. Phys. Chem. C*, 2018, **122**, 23165; (*e*) M. Nakagawa and T. Kawai, *J. Am. Chem. Soc.*, 2018, **140**, 4991–4994.

8 S. Sun and H. Zeng, *J. Am. Chem. Soc.*, 2002, **124**, 8204–8205.

9 (*a*) C. R. Vestal and Z. J. Zhang, *J. Am. Chem. Soc.*, 2003, **125**, 9828–9833; (*b*) M. Aslam, E. A. Schultz, T. Sun and T. Meade, *Cryst. Growth Des.*, 2007, **7**, 471–475.

10 (*a*) M. P. Morales, S. Veintemillas-Verdaguer, M. I. Montero, C. J. Serna, A. Roig, L. Casas, B. Martínez and F. Sandiumenge, *Chem. Mater.*, 1999, **11**, 3058–3064; (*b*) T. Fried, G. Shemer and G. Markovich, *Adv. Mater.*, 2001, **13**, 1158–1161; (*c*) C. Ravikumar and R. Bandyopadhyaya, *J. Phys. Chem. C*, 2011, **115**, 1380–1387; (*d*) S. Sun, H. Zeng, D. B. Robinson, S. Raoux, P. M. Rice, S. X. Wang and G. Li, *J. Am. Chem. Soc.*, 2004, **126**, 273–279.

11 Y.-C. Chang and D.-H. Chen, *J. Colloid Interface Sci.*, 2005, **283**, 446–451.

12 Y. Imura, C. Morita and T. Kawai, *New J. Chem.*, 2013, **37**, 3607–3611.

